

# Effects of Fouled Ballast Layer on Railway Bridge Vibrations

Saeid Farsi \*  
University of South Carolina  
Columbia, USA

Hossein Asgari  
Practice Railway Expert  
Tehran, Iran

**Abstract:** This research investigates the influence of fouled ballast layers on vibrations in railway bridges. The research introduces and validates a Train-Track-Bridge Interaction (TTBI) model designed to investigate the dynamic response of a bridge under different degrees of ballast contamination. The primary focus is on analysing midpoint deflection, velocity, and acceleration during the traversal of a train. The study reveals substantial improvements in track stability with a 37.5% reduction in bridge deflection as ballast stiffness increases from 40 to 70 MPa. Conversely, contaminated ballast leads to a 35.7% increase in midpoint velocity and a doubled vibration range when ballast stiffness rises from 40 to 80 MPa, highlighting the importance of considering ballast conditions in railway infrastructure design. Additionally, there is a significant 28.6% variation in maximum acceleration with increasing fouling rates, particularly impacting the bridge during the crossing of the 2<sup>nd</sup> wagon. The findings underscore the critical necessity for robust maintenance strategies to address fouling issues and ensure the long-term health and performance of railway bridges.

**Keywords:** ballast contamination; bridge vibration; railway track; train-track interaction; fouled ballast; track stiffness

## 1. INTRODUCTION

Railway infrastructure is a critical component of modern transportation systems, efficiently connecting regions and facilitating the smooth movement of goods and passengers. The integrity and stability of railway bridges, crucial elements in this extensive network, are essential to ensuring safe and reliable operations [1]. Among the various factors influencing the structural dynamics of railway bridges, the condition of the ballast layer emerges as a significant consideration. The ballasted layer, constructed with uniform and angular particles, plays a crucial role in distributing train loads effectively to the bridge [2]. The effective functioning of the ballast layer guarantees the secure transit of heavy freight trains across the railway network. Ballast serves various roles, including its substantial impact on the dynamic interaction between a rail bridge and a moving load, particularly in terms of damping and load distribution [3]. While its role in providing stability, facilitating drainage, and distributing loads is well-established, its impact on the vibrations experienced by railway bridges remains a subject of evolving exploration [4]. The fouling of ballast over railway bridges, influenced by environmental factors and operational aspects, is a complicated process. Elements like wind, rain, and weather conditions contribute to the introduction of dust, dirt, and debris into the ballast. In addition, the regular passage of trains over the bridge generates wear and tear on the tracks, producing fine particles that settle into the ballast. The spills of substances such as oil and chemicals, and improper maintenance practices further contribute to the accumulation of contaminants. The result is a fouled superstructure, as shown in Figure 1. Consequently, ballast fouling becomes an inevitable aspect of real-world track operation, adversely affecting damping features and leading to severe vibrations as trains cross over bridges [5]. As a result, ballast will be stiffer, and the sleeper may be suspended over the ballast layer which

leads to the appearance of gaps. Consequently, the ballast becomes more rigid, causing the sleeper to potentially be suspended over the ballast layer, leading to the emergence of gaps. Lundqvist and Dahlberg [6] investigated the consequences of separating between sleeper and ballast. The findings indicated a 70% augmentation in the interaction force between supported sleepers and the ballast. Furthermore, Naseri and Mohammadzadeh [7] demonstrated that in the case of an unsupported sleeper-group within the 2/8 and 5/8 span of the bridge, the acceleration of the bridge reaches its maximum. Additionally, the maximum load on the deck of the bridge experiences an increase ranging from 45 to 60%. Esmaili [8] demonstrated that with a rise in ballast fouling percentage from 0 to 62.7%, there was an approximately 43% increase in maximum acceleration, accompanied by a reduction of approximately 68% in maximum displacement. The fouling of ballast additionally diminishes the resistance from the ballast layer to the sleeper, leading to track instability and irregular track geometry [9]. Regarding bridge performance, although prior research has thoroughly investigated the dynamic response of bridges to moving loads [10-12], there has been limited exploration into the specific effects of a contaminated ballast layer on bridge vibrations. Recognizing these effects is essential for improving the comprehension of the challenges introduced by ballast fouling.

This study examines the complicated interactions between the fouled ballast layer, the track, and the bridge, aiming to identify the dynamics contributing to vibrations on railway bridges. By conducting a comprehensive examination of the impact of ballast fouling, the research seeks to provide valuable insights for engineers, researchers, and practitioners involved in railway infrastructure planning, construction, and maintenance

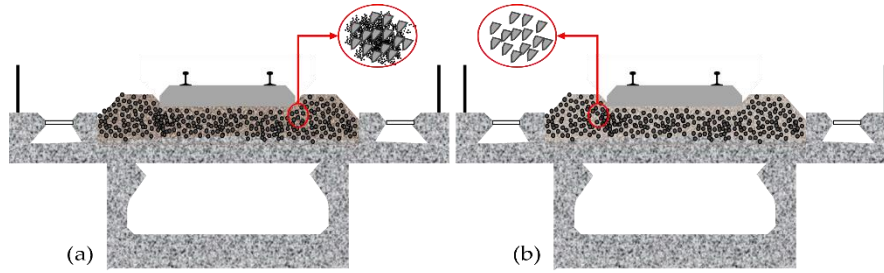


Figure. 1 Ballast fouling over the bridge a) fouled ballast and b) clean ballast

## 2. MODELING OF TRAIN-TRACK-BRIDGE INTERACTION (TTBI)

This section establishes the foundational framework for the analysis of the intricate dynamics involved in TTBI. It serves as the basis for subsequent analysis, presenting a structured approach to comprehending the intricate interactions within the TTBI system.

### 2.1 Vehicle model

To model the train, three main parts of each vehicle, including one car-body, two bogies, and four wheelsets are connected by linear spring-viscous dashpot elements. The detailed descriptions of vehicle modeling and the proposed assumptions are as follows: 1) the car-body is modeled as a rigid beam, regardless of the bending mode shapes, that can have vertical and pitching movements, and is connected to the rear and front bogies by the secondary spring-damper set. 2) the bogie with two degrees of freedom, similar to the car-body model, is linked to the wheels by the primary spring-damper set. 3) each wheelset is represented as a mass and only the vertical bouncing motion is considered. For a simplified though still accurate enough analysis, it is assumed the performance of vehicle elements is entirely independent of each other. This assumption makes it possible to generate vehicle matrices mentioned in previous studies[13].

### 2.2 Track model

In the study of train-track-bridge interaction, the track system is one of the main parts that play a significant influence on the level of vibrations on the bridge surface [14]. Therefore, maintaining the quality of track in the rail transport system, especially in the bridge zone, is inevitable. To model the track system, a finite element model of beam-sleeper-ballast has been used. Yuan et al. [15] presented the detailed descriptions of the rail-sleeper force.

### 2.3 Bridge model

In this study, the bridge model is represented as a simply supported Timoshenko beam which has been widely used to study the bridge dynamic under railway traffic. An analytical approach is considered for bridge modeling based on the Direct Stiffness Method (DSM), which is suitable for short span bridges. This model allows us to utilize a high computation efficacy model and versatile technique in TTB numerical analysis [14]. In this study, only vertical and rotational degrees of freedom are considered. Also it is assumed that throughout the analysis, there is no separation between the sleeper and the bridge surface [16]. The stiffness and mass matrices for the Timoshenko beam element are obtained as follows:

$$m_{mn} = \int_0^l m_{(x)} \xi_m \xi_n dx, \quad m, n = 1:4 \quad (1)$$

$$k_{mn} = \int_0^l EI_{(x)} \frac{d^2 \xi_m}{dx^2} \frac{d^2 \xi_n}{dx^2} dx, \quad m, n = 1:4 \quad (2)$$

In Eq. 4 and 5,  $m$  and  $n$  are the degrees of freedom.  $\xi_i$  can be defined as:

$$\xi_i = \begin{cases} \kappa(2x^3 - 3x^2l + l^3) & i = 1 \\ \kappa(-2x^3 + 3x^2l) & i = 2 \\ \kappa(-x^3l + x^2l^2(2 + \phi/2) - xl^3(1 + \phi)) & i = 3 \\ \kappa(-x^3l + x^2l^2(1 - \phi/2)) & i = 4 \end{cases} \quad (3)$$

Where

$$\kappa = 1/(l^3 (1 + 24\alpha(1 + \nu)(r/l)^2)) \quad (4)$$

is the constant to consider the bridge shear stiffness. Besides, the parameters of  $\nu$ ,  $r$ , and  $l$  represent Poisson's ratio, the radius of gyration of the bridge cross-section, and the length of the Timoshenko beam element, respectively.  $\alpha$  is shear area coefficient that for the solid section is 6/5 [17]. The damping matrix, is obtained from Rayleigh damping by the linear combination of mass matrix and stiffness matrix of the bridge[18].

### 2.4 Wheel-rail interaction

To calculate the wheel-rail force, a mutual iterative algorithm needs to be adopted between moveable and immoveable subsystems. The interaction between the rail and the wheels is utilized to couple the equations of the moveable and immoveable subsystems. Based on Hertz's non-linear theory, the corresponding contact forces are calculated. According to the Hertzian contact theory, the interaction force between wheel and rail at location  $x$  can be expressed as:

$$F_{r/wi}(t) = \begin{cases} c_h |y_x|^{1.5} & y_x \leq 0 \\ 0 & y_x > 0 \end{cases} \quad (5)$$

Where  $y_x$  represent the relative displacements of the wheelset and rail in the coordinate  $x$ .  $c_h$  is the nonlinear Hertzian contact coefficient which depends on the material properties and the wheel and rail profiles [19].

## 3. METHODOLOGY OF SOLUTION

Iterative algorithms serve as highly accurate numerical modeling techniques for individual subsystems, employing a two-step calculation process. As depicted in Figure 2, initially, the dynamic behavior of a vehicle model is analyzed, and subsequently, the accumulated nonlinear wheel-rail interaction forces are applied to a track-bridge analysis. A

comprehensive procedural outline is available in [7]. In order to improve efficiency and reduce computation time, all time-dependent coefficients and interaction elements of the moveable and immovable subsystem's matrices are expressed in the force vector in order to make the algorithm more efficient. Moreover, in the time domain algorithm presented here, the position of the moveable subsystem is updated at each time step, and the response of both subsystems is calculated. For this purpose, the time interval between consecutive steps should be considered small to achieve high accuracy [20]. The dynamic equations for both subsystems are solved using Newmark's finite difference scheme, a widely adopted approach in engineering practices.

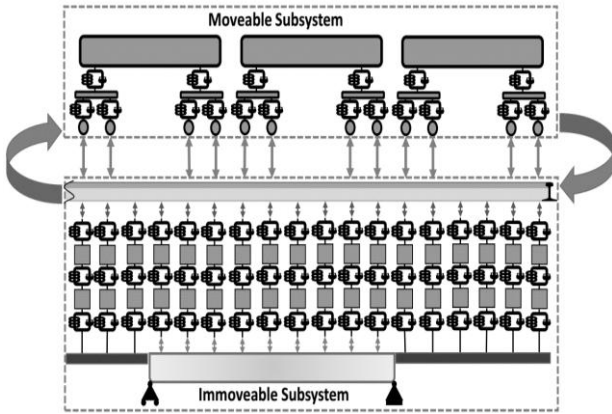


Figure 2. Presented TTBI model.

#### 4. VERIFICATION

To demonstrate the effectiveness of the proposed methodology, a case study derived from [21] is chosen. The model is shown in Figure 3. The vehicle properties are chosen from those for the Shinkansen train in [22]. The train speed is assumed to be 100 km/h, which crosses the bridge at a constant speed. The track is modeled using a continuous Euler-Bernoulli beam on a series of horizontal and vertical spring-dampers. The results are compared to those from the literature [21].

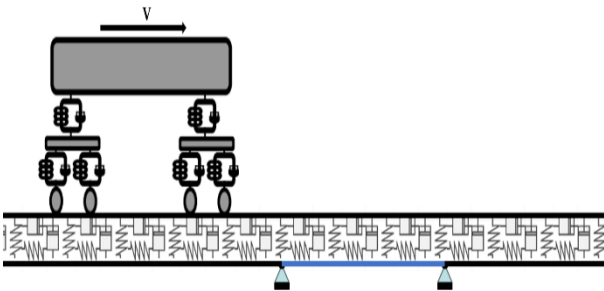


Figure 3. Schematic of the employed TTBI model for verification.

The graphical representation in Figure 4 illustrates the dynamic response, showcasing the acceleration and displacement of the bridge. The observations drawn from the figure indicate a notable similarity between the outcomes obtained through the numerical methodology employed in this study and those documented in [21]. The graphical representation highlights the agreement and consistency observed in the results, reinforcing the reliability of the

computational approach applied in this research and affirming its consistency with established findings in the literature.

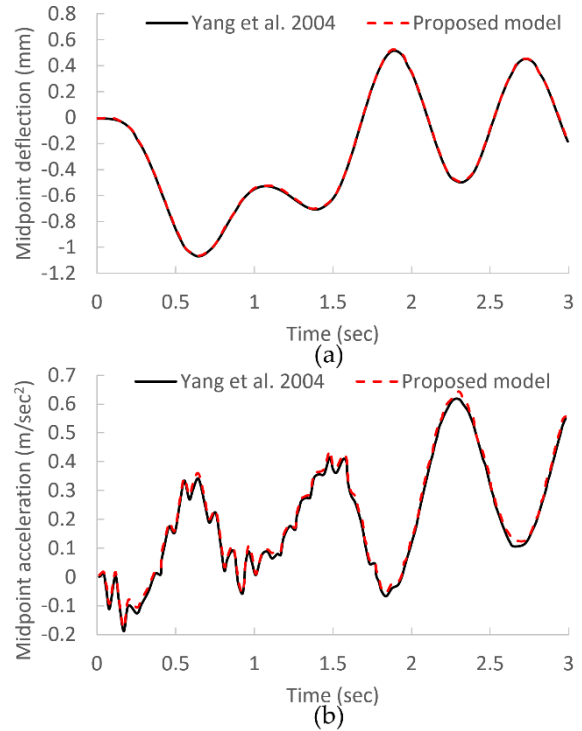


Figure 4. . Dynamic response of bridge (a) midpoint displacement (b) midpoint acceleration

#### 4.1 Results and discussion

The model presented in this paper is employed for the assessment of a 16-meter single-span railway bridge, with mechanical parameters provided in [23]. The study incorporates an ICE train model consisting of three wagons, each carrying an average static load of 100 kN, traveling over a track simulated with a three-layered rail-sleeper-ballast model. Reference [7] outlines the specific characteristics of both the train and the track. The ballast shear interlocking is modeled using the proposed equation in [24]. The analysis assumes a constant train speed of 90 km/h throughout the entire TTBI analysis. The ballast layer is modeled to account for varying levels of contamination with sand, with reference [1] indicating a typical ballast stiffness of 40 MPa, which can increase to 70 MPa in the case of sand contamination. To assess the performance of the bridge under different track stiffness resulting from sand contamination, the specified range of ballast stiffness is utilized. The outcomes of the TTBI model are detailed in the subsequent sections.

##### 4.1.1 Midpoint deflection

Figure 5 depicts the midpoint deflection of the bridge during the passage of the train, considering four different cases with ballast stiffnesses of 40, 50, 60, and 70 MPa in this model. The image illustrates that as the ballast stiffness increases, the midpoint deflection decreases. Specifically, comparing the case with a ballast stiffness of 70 MPa to that with 40 MPa, the bridge deflection decreases from 0.48 mm to 0.30 mm, indicating a 37.5% reduction in bridge deflection. Furthermore, the rate of reduction or the difference between each two consecutive cases diminishes as the ballast stiffness

increases. The most significant difference occurs when the middle wagon is on the track, primarily due to the axle load distances between the 2<sup>nd</sup> and the adjacent axles from the 1<sup>st</sup> and 3<sup>rd</sup> wagon.

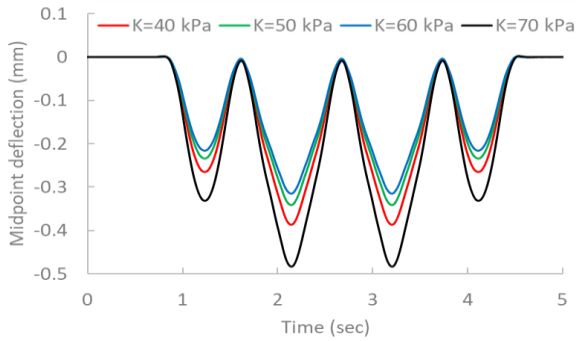


Figure 5. Bridge midpoint deflection in different cases of ballast stiffness

#### 4.1.2 Midpoint velocity

Figure 6 illustrates the bridge velocity at the midpoint as the train traverses the span. The graph clearly shows that contaminated ballast results in higher levels of vibration in the bridge. The midpoint velocity increases from 0.9 to 1.4 mm/sec as the ballast stiffness varies from 40 to 80 MPa, representing approximately a 35.7% increase in the bridge velocity. Additionally, the range of vibration expands from  $\pm 0.9$  mm/sec to  $\pm 1.4$  mm/sec, indicating that the range is twice the difference between the maximum vibrations. This observed behavior in bridge vibration, influenced by different ballast stiffness levels, underscores that as the track becomes stiffer, the train-induced vibration has a more significant impact on the bridge performance.

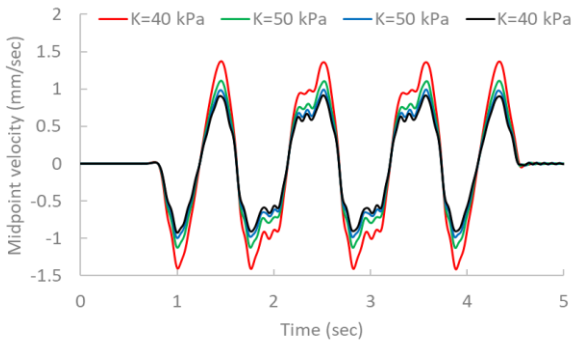


Figure 6. Bridge midpoint velocity in different cases of ballast stiffness.

#### 4.1.3 Midpoint acceleration

Bridge acceleration is a crucial factor that profoundly impacts the overall health of a bridge, influencing both short-term risks like abrupt collapse and long-term performance concerns such as fatigue. As depicted in Figure 7, this study presents the midpoint acceleration time history of the bridge. The findings reveal that with an increase in the fouling rate of the ballast, the acceleration amplitude significantly rises from 14 mm/sec<sup>2</sup> to 18 mm/sec<sup>2</sup>. This alteration results in approximately a 28.6% variation in the maximum acceleration

of the bridge. The heightened response of the bridge is particularly prominent in the central portion of the graph, where the 2<sup>nd</sup> wagon crosses over the bridge. This emphasizes the influence of axle load distance in this scenario, especially when it is closer to the adjacent axles.

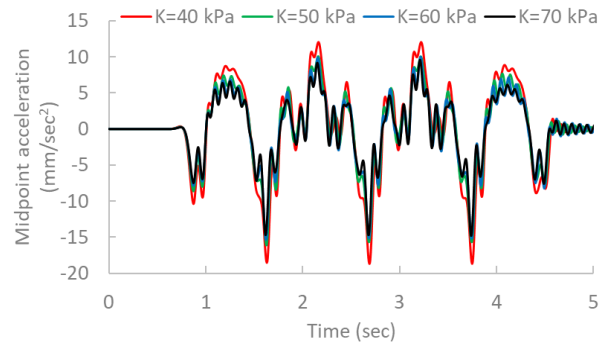


Figure 7. Bridge midpoint acceleration in different cases of ballast stiffness.

## 5. CONCLUSION

This paper particularly examined the bridge dynamic performance in the different scenarios of ballast fouling. To achieve this goal an FEM model of TBBI was presented. The model was verified with the results of the literature which showed good agreements. Then the model is utilized to evaluate the bridge performance in the for cases of ballast stiffness. The results of this paper can be summarized as follows:

1. The research established a distinct relationship between ballast stiffness and the midpoint deflection of the bridge during train passages. Specifically, there is a 37.5% reduction in bridge deflection as ballast stiffness increases from 40 to 70 MPa. This highlights the crucial contribution of elevated ballast stiffness in promoting track stability, mitigating vibrations, and enhancing the overall performance of the bridge.
2. Ballast contamination significantly increases bridge vibration levels. As ballast stiffness rises from 40 to 80 MPa, the midpoint velocity experiences a 35.7% increase, and the vibration range doubles. This underscores the critical importance of factoring in ballast conditions in the design and maintenance of railway infrastructure to efficiently manage and control bridge vibrations.
3. Higher fouling rates lead to a notable 28.6% variation in maximum acceleration, particularly affecting the bridge during the passage of the 2<sup>nd</sup> wagon. This highlights the critical necessity for strong maintenance strategies to tackle fouling issues and guarantee the enduring health and performance of railway bridges.

## 6. REFERENCES

- [1] Touqan, M., M.H. El Naggat, and T.D. Stark. 2022 In-situ performance assessment of track superstructure on fouled railroad. *Transportation Geotechnics*. 32: p. 100695.

- [2] Naseri, R. 2020 Consequences of rail surface local irregularities on railway concrete bridge vibrations. Iran University of Science and Technology (IUST).
- [3] Aloisio, A., M.M. Rosso, and R. Alaggio, 2022. Experimental and analytical investigation into the effect of ballasted track on the dynamic response of railway bridges under moving loads. *Journal of Bridge Engineering*. 27(10): p. 04022085.
- [4] Farsi, S., M. Esmaili, and R. Naseri. 2024. Effect of rock strength on the degradation of ballast equipped with under sleeper pad using discrete element method. In ASME/IEEE Joint Rail Conference. American Society of Mechanical Engineers.
- [5] Esmaili, M., P. Aela, and A. Hosseini, 2017. Experimental assessment of cyclic behavior of sand-fouled ballast mixed with tire derived aggregates. *Soil Dynamics and Earthquake Engineering*. 98: p. 1-11.
- [6] Lundqvist, A. and T. Dahlberg, 2005. Load impact on railway track due to unsupported sleepers. *Proceedings of the Institution of Mechanical Engineers, Part F: Journal of Rail and Rapid Transit*. 219(2): p. 67-77.
- [7] Naseri, R., and S. Mohammadzadeh, 2020. Nonlinear Train-Track-Bridge Interaction with Unsupported Sleeper Group. *International Journal of Railway Research*. 7(1): p. 11-28.
- [8] Esmaili, M., J.A. Zakeri, and S.A. Mosayebi, 2014. Effect of sand-fouled ballast on train-induced vibration. *International Journal of Pavement Engineering*. 15(7): p. 635-644.
- [9] Ngamkhanong, C., et al., 2021. Evaluation of lateral stability of railway tracks due to ballast degradation. *Construction and Building Materials*. 278: p. 122342.
- [10] Liu, S., et al., 2023. Dynamic response analysis of multi-span bridge-track structure system under moving loads. *Mechanics Based Design of Structures and Machines*. 51(10): p. 5669-5687.
- [11] Melo, L.T., et al., 2020. Dynamic analysis of the train-bridge system considering the non-linear behaviour of the track-deck interface. *Engineering Structures*. 220: p. 110980.
- [12] Yau, J. and S. Urushadze, 2024. Resonance reduction for linked train cars moving on multiple simply supported bridges. *Journal of Sound and Vibration*. **568**: p. 117963.
- [13] Naseri, R., S. Mohammadzadeh, and D.C. Rizos, 2024. Rail surface spot irregularity effects in VTI simulations of train-track-bridge interaction. *Journal of Vibration and Control*.
- [14] Zhai, W., et al., 2019. Train-track-bridge dynamic interaction: a state-of-the-art review. *Vehicle System Dynamics*. 57(7): p. 984-1027.
- [15] Yuan, Z., et al., 2021. Vibration-based damage detection of rail fastener clip using convolutional neural network: Experiment and simulation. *Engineering Failure Analysis*. 119: p. 104906.
- [16] Xia, H., N. Zhang, and W. Guo, 2018. *Dynamic Interaction of Train-Bridge Systems in High-Speed Railways*. Springer.
- [17] Gavin, H.P., 2014. Structural element stiffness, mass, and damping matrices. CEE 541. *Structural Dynamics*.
- [18] Zhu, Z., et al., 2017. A hybrid solution for studying vibrations of coupled train-track-bridge system. *Advances in Structural Engineering*. 20(11): p. 1699-1711.
- [19] Du, X., Y. Xu, and H. Xia, 2012. Dynamic interaction of bridge-train system under non-uniform seismic ground motion. *Earthquake Engineering & Structural Dynamics*. 41(1): p. 139-157.
- [20] Xu, L. and W. Zhai, 2019. A three-dimensional model for train-track-bridge dynamic interactions with hypothesis of wheel-rail rigid contact. *Mechanical Systems and Signal Processing*. 132: p. 471-489.
- [21] Yang, Y.-B., et al., 2004. *Vehicle-bridge interaction dynamics: with applications to high-speed railways*. World Scientific.
- [22] Wakui, H., et al., 1995. Dynamic interaction analysis for railway vehicles and structures. *Doboku Gakkai Ronbunshu*. 1995(513): p. 129-138.
- [23] Yau, J.-D., Y.-B. Yang, and S.-R. Kuo, 1999. Impact response of highspeed rail bridges and riding comfort of rail cars. *Engineering structures*. 21(9): p. 836-844.
- [24] Heydari, H., N. Khanie, and R. Naseri, 2023. Formulation and Evaluation of the Ballast Shear Interlocking Coefficient based on Analytical, Experimental, and numerical Analyses. *Construction and Building Materials*. 406: p. 133457.